Effects of different amosite preparations on macrophages, lung damages, and autoimmunity

Impact of short and long amosite fibers on human macrophages, fibrosis and autoimmunity in mouse models

Alain Lescoat
Universite de Rennes 1
Riccardo Leinardi
Catholic University of Louvain: Universite Catholique de Louvain
Kevin Pouxvielh
Universite de Rennes 1
Yousof Yacoub
Catholic University of Louvain: Universite Catholique de Louvain
Marie Lelong
Universite de Rennes 1
Amandine Pochet
Catholic University of Louvain: Universite Catholique de Louvain
Erwan Dumontet
CHU Rennes: Centre Hospitalier Universitaire de Rennes
Nessrine Bellamri
Universite de Rennes 1
Erwan Le Tallec
CHU Rennes: Centre Hospitalier Universitaire de Rennes
Cristina Pavan
University of Turin: Universita degli Studi di Torino
Francesco Turci
University of Turin: Universita degli Studi di Torino
Christophe Paris
CHU Rennes: Centre Hospitalier Universitaire de Rennes
François Huaux
Catholic University of Louvain: Universite Catholique de Louvain
valerie Lecureur (✉ valerie.lecureur@univ-rennes1.fr)
University of Rennes 1 https://orcid.org/0000-0002-8606-4755

Research Article

Keywords: Amosite fibers, Asbestos, Autoimmunity, Efferocytosis, Lung fibrosis, Macrophages

Posted Date: February 8th, 2023

DOI: https://doi.org/10.21203/rs.3.rs-2504079/v1

Abstract

Although epidemiological studies have suggested an association between asbestos exposure and systemic autoimmunity, the underlying mechanisms are poorly understood. Short asbestos fibers are often considered less harmful than long fibers but such a statement is still a matter of debates. This study aimed to compare the effects of short (SFA) and long (LFA) amosite fiber exposure on lung damage, autoimmunity and macrophage phenotype. Four months after lung exposure to 0.1 mg of fibers, BAL levels of lactate dehydrogenase, free DNA, CCL2, TIMP-1 and immunoglobulins A of LFA-exposed C57Bl/6 mice were increased when compared to fluids from control- and SFA-exposed mice. Effects in LFA-exposed mice were associated with lung fibrosis and autoimmunity including anti-double-strand DNA antibody production. Human monocyte-derived macrophages (MDMs) exposed to SFA or LFA at 20 µg/cm2 have a pro-inflammatory phenotype characterized by a significant increase of TNFα and IL-6 secretion. A decrease of efferocytosis capacities was also noted after SFA and LFA, whereas macrophage abilities to phagocyte fluorescent beads were unchanged when compared to control MDMs. SFA exposure induced IL-6 secretion and reduced the percentage of MDMs expressing MHCII and CD86 markers involved in antigen and T-lymphocyte stimulation. By contrast, NLRP3 inflammasome activation, evaluated through quantification of caspase-1 activity and IL-1β secretion is rather associated to LFA than SFA exposure. Our results demonstrated that only long-term exposure to LFA has induced significant lung damages and autoimmune effects supporting a worsened health effects of LFA in comparison to SFA.

Introduction

Asbestosis remains a public health concern as about 125 million of people in the world are still exposed to asbestos fibers at the workplace, although its use is banned in several countries. Indeed, the detrimental health effects of asbestos including mesothelioma, lung cancer and fibrosis, can appear a long time after exposure. Beyond such pulmonary disorders, the association between asbestos exposure and autoimmune diseases, characterized by autoantibodies production, has also been reported (Marczynski et al. 1994a; Pfau et al. 2014; Janssen et al. 2022). Although dust-related autoimmunity is classically considered associated with chronic occupational exposure, acute occupational exposure and non-occupational exposure may also induced autoimmunity (Webber et al. 2015; Cavalin et al. 2022). However, autoimmune effects of asbestosis as still poorly understood as compared to their effects on fibrosis or cancer. Nevertheless, exposure to amphiboles such as amosite and crocidolite, the most common fibers, increases the production of autoantibodies whereas an exposure to serpentines such as chrysotile does not (Zebedeo et al. 2014), demonstrating that the physico-chemical nature of the fibers is crucial to initiate systemic autoimmunity.

Beyond the nature (amphibole versus serpentine) of asbestos fibers, bio-persistence and size also represent key parameters of their toxicity and health effects. Currently, legislation on asbestos fibers focuses on long asbestos fibers which are characterized by the World Health Organization (WHO) as follows: Length (L) ≥ 5 µm, diameter (D) <3 µm and L/D ratio > 3. However, indoor air samples, collected

in normal building occupancy and usage, contain a high proportion (usually more than 70%) of short asbestos fibers (Boulanger et al. 2014) characterized by a shorter length (< 5 µm, with D< 3 µm and L/D ratio >3) as compared to long fibers. Even if short asbestos fibers are often considered less harmful than long fibers, such statement is still a matter of debates. Therefore, short asbestos fiber pathogenicity still needs to be addressed, especially considering their high proportion in air, which may lead to a non-negligible concentration and thereof exposure.

The major lung cells in contact with inhaled asbestos fibers are epithelial cells and alveolar macrophages. They can recognize fibers through scavenger receptors such as MARCO (Murthy et al. 2015) and phagocyte them depending on their size. Indeed, the short enough fibers (< 5 µm in length) may be more easily cleared than the long fibers (> 10 µm), which lead to an imperfectly engulfment of fibers called “frustrated phagocytosis” favoring alveolar macrophage cell death, the release of reactive oxygen and nitrogen species and the recruitment of inflammatory cells. This chronic inflammation is also promoted by asbestos-induced activation of the NOD-like receptor family domain pyrin domain containing 3 (NLRP3) inflammasome triggering the production of the inflammatory interleukin-1β (IL-1β) cytokine (Dostert et al. 2008). Asbestos-induced chronic inflammation in turn triggers the activation of fibroblasts and collagen deposition.

Despite some epidemiological studies suggesting an association between asbestos and autoimmunity, characterized by the production of anti-nuclear autoantibodies (ANA) (Pfau et al. 2005; Bunderson-Schelvan et al. 2011; Janssen et al. 2022), the underlying mechanisms are poorly understood. By contrast, the association between respirable crystalline silicate and development of systemic autoimmune diseases characterized by the production of ANA, is well endorsed (Parks et al. 1999; Pollard 2016). Such effects may occur through cellular debris accumulation due to particle-induced apoptosis and a defect of their clearance in silica-exposed macrophages, leading to the release of intracellular components in the extracellular medium (Lescoat et al. 2020a). Efficient phagocytosis of apoptotic bodies by macrophages, a process called “efferocytosis” participates in immune silencing (Kawano and Nagata 2018), by preventing this release of intra-cellular antigens, including self-DNA and DNA associated proteins. Efferocytosis is impaired by silica exposure in vitro and in vivo, and such impairment of immune silencing could directly participate in silica-induced autoimmunity. Indeed, the release of intracellular components due to defective efferocytosis and their persistence in the extracellular medium can induced autoimmunity as such intracellular antigens can be recognized as autoantigens by adaptive immunity inducing the production of ANA, such as anti-dsDNA antibodies. Uncleared intracellular components resulting from defective efferocytosis are also recognized by antigen-presenting cells and innate immune cells as damage-associated molecular patterns inducing their persistent activation in a pro-inflammatory state. The impact of asbestos exposure on efferocytosis and the links with autoimmunity in this context remains to be determined.

This study was designed to compare the effects of short and long amosite fibers at the lung and systemic levels with a focus on immune responses including autoimmunity and on macrophage function by using in vivo, in vitro and ex vivo approaches.

Materials And Methods

Mineral Fibers

Short fiber amosite (SFA) and long fiber amosite (LFA), kindly provided by F. Turci (Turin, Italy) originated from South Africa. The length range of LFA was 2-100 µm with more than 30% of fibers longer than 5 µm. SFA were obtained by grinding of LFA and its length range was 1-10 µm, with less than 1% fibers longer than 5 µm. The diameter distribution ranged between 0.2-1.5 µm and was similar for both fibers (Davis et al. 1986; Tomatis et al. 2010). All samples were thermally treated at 200°C for 3 h to remove any possible trace of endotoxin and suspensions were prepared by sonication and manual vortexing in sterile Phosphate-buffered saline (PBS) or water for in vivo and in vitro experiments, respectively.

Chemicals and reagents

Human recombinant cytokines IFN ，IL-4 and IL-13 were purchased from Peprotech (Neuilly sur Seine, France) and human recombinant M–CSF was obtained from Miltenyi Biotec SAS (Paris, France). Lipopolysaccharide (LPS) from E.coli (serotype: 055:B5) and z-VAD-FMK were purchased from Sigma-Aldrich (St-Quentin Fallavier, France) and MedChemExpress (Clinisciences, Nanterre, France), respectively. Stock solutions human recombinant cytokines were prepared in sterile distilled water containing 0.1% bovine serum albumin. Z-VAD-FMK was dissolved in DMSO and control culture received the same dose of DMSO than their treated counterparts, without exceeding 0.2% (vol/vol).

Animals

Female C57BL/6 mice weighing 20 gr, used at 8 weeks of age, were purchased from Janvier SAS (St Berthevin, France). Animals were kept with sterile rodent feed and acidified water, and housed in positive-pressure air-conditioned units (25 °C, 50% relative humidity) on a 12 h light/dark cycle. After acclimatization, the animals were exposed by intra-tracheal instillation to short or long amosite fibers (0.1 mg) suspended in a volume of 0.5 ml of PBS-BSA. Vehicle controls were injected with an equal volume of PBS-BSA. Mice were then euthanized 4 months (120 days) after particle administration with an intraperitoneal injection of 12 mg sodium pentobarbital (Certa, Braine-l'Alleud, Belgium).

Broncho-alveolar lavage and lung sampling

The broncho-alveolar lavage (BAL) was performed by cannulating the trachea and infusing the lungs with 4x with 1 ml 0.9% NaCl. The BAL fluid was centrifuged 280 g, 4 °C, 10 min using a 5804R centrifuge (Eppendorf, Hamburg, Germany), and the cell-free supernatant was used for biochemical measurements. After resuspension of the pellet in PBS, total BAL fluid cells were counted (at least 200 cells) in Turch (crystal violet 1%, acetic acid 3%), and then pelleted onto glass slides by cyto-centrifugation for differentiation by light optical microscopy, after Diff-Quick staining (Baxter, Lessines, Belgium). Total proteins and lactate dehydrogenase (LDH) activity were assessed on BAL fluid as previously described (Arras et al. 2001). BAL fluid content of double-stranded DNA (dsDNA) was measured using Quant-iT PicoGreen dsDNA reagent (Invitrogen, Carlsbad, USA), according to the manufacturer's protocol.

Quantification of total lung collagen and BAL cytokines

Collagen deposition was estimated by measuring hydroxyproline (OH-proline) content in lung homogenates and tissue inhibitor of metalloproteinase (TIMP-1) content in BAL fluids. Hydroxyproline was assessed by high-pressure liquid chromatography analysis on hydrolyzed lung homogenates (6 N HCl at 108° C during 24 h) as previously described (Biondi et al. 1997). TIMP-1 levels were assessed by ELISA (R&D Systems, Minneapolis, USA). The following ELISA were performed on BAL fluids according to manufacturers' instructions: CCL2 were investigated using a DuoSet ELISA kit (R&D Systems, Minneapolis, USA); total Ig-G, Ig-A and Ig-M were measured using an Invitrogen Uncoated ELISA kit (ThermoFischer Scientific, Courtaboeuf, France).

Lung Histology

Lungs were instilled and perfused with 0.9% NaCl and superior-left lung lobe was fixed in 3.6% formaldehyde solution (Sigma-Aldrich, Saint Louis, USA) for one night. Sections embedded in paraffine were stained with hematoxylin and eosin (H&E, nucleus and cytoplasm staining). Images were acquired with a slide scanner SCN400 (Leica, Diegem, Belgium) and processed with Tissue Image Analysis 2.0 (Leica).

Preparation of Human Monocyte-Derived Macrophages (MDMs)

As alveolar macrophages, and especially those derived from monocytes, seem play a key role in asbestos-induced lung fibrosis development (Joshi et al. 2020), the model of human monocyte-derived macrophages is well adapted to study and compare the cellular effects of short and long asbestosis fibers.

Patients exposed to silicate particles and healthy donors (HD): Peripheral blood mononuclear cells were obtained from HD or patients exposed to silica particles through Ficoll (Eurobio, Les Ulis, France) gradient centrifugation. Blood buffy coat from HD were provided by the Etablissement Français du sang (Rennes, France) after their consent. Patients exposed to silica from the Occupational Health and Occupational Pathology Service of Rennes University hospital were consecutively included after written informed consent. This study was approved by the local ethics committees (Committees for protection of persons approval Ile de France 5, N°2020-A01990-39).

Differentiation of monocytes in MDMs and treatment: Monocytes, selected after a 1-h adhesion step, were differentiated into MDM for 6 days using M–CSF (50 ng/ml) in RPMI 1640 medium GlutaMAX (Gibco, Life technologies SAS, Courtaboeuf, France) supplemented with antibiotics (20 IU/ml penicillin and 20 µg/ml streptomycin (ThermoFisher Scientific) and 10% heat inactivated fetal bovine serum (FBS, Lonza, Levallois-Perret, France), as previously described (Lescoat et al. 2020b). After 6 days, the supernatant of cells was removed and replaced with medium containing 5% of heat-inactivated FBS and M–CSF (10 ng/ml). These cells corresponding to M0-MDMs were then exposed to SFA or LFA from 0 to 50 ng/cm^2. In some case, M0-MDMs were pre-incubated to 10 ng/ml of LPS in the presence or not of 10

μM of z-VAD-FMK before amosite fibers. According to experiments, conditioned media were removed and stocked at −20 °C for ELISA analysis whereas the cells were washed and harvested for RNA extraction or flow cytometry analysis.

Evaluation of cell viability, cytokine/chemokine levels and Caspase-1 activity

Cell viability was assessed with CyQUANT assay (in vitrogen, Thermofisher). MDMs plated at $2x10^5$ cells/cm^2 were exposed at different concentrations of fibers from 0 to 50 μg/cm^2) for 4 h or 24 h. After particle exposure, CyQUANT was added to MDMs in complete medium, incubated for 1 h at 37°C and read on using appropriate wavelengths (485/540 nm) a spectrofluorimeter SPECTROStar OMEGA (BMG Labtech, Champigny s/Marne, France).

Levels of human IL-1β, IL-6, IL-8, and TNFα secreted in MDM culture media were quantified by ELISA using specific Duoset ELISA development system kits (R&D Systems, Minneapolis, MN, USA).

Caspase-1 activity was quantified by luminescence using the Caspase-Glo 1 inflammasome assay according to the recommendations of providers (Promega, Charbonnières-les-Bains, France) on a Enspire 2300 luminometer (Perkin-Elmer, Waltham, MA, USA).

Reverse transcription-quantitative polymerase chain reaction (RTqPCR) experiments

Total RNAs were extracted from cells with Nucleospin RNA extraction Kit (Macherey-Nagel) and reverse transcribed using the High-Capacity cDNA Reverse Transcription Kit (Applied Biosystems, ThermoFisher Scientific). qPCR assays were next performed using the fluorescent dye SYBR Green methodology and a CFX384 Real-Time PCR detector (Bio-Rad Laboratories, Marnes-la-Coquette, France). The KiCqStart® SYBR® Green primers for human and mouse cDNA were provided by Sigma-Aldrich. The specificity of amplified genes was evaluated using the comparative cycle threshold method (CFX Manager Software). These mean Cq values were used to normalize the target mRNA concentrations to those of the 18S ribosomal protein by the $2^{(-\Delta\Delta Cq)}$ method.

Cell surface receptors and markers analyses by flow cytometry

Phenotypic analysis of MDMs was performed using flow cytometric direct immunofluorescence. After washing and plastic detachment using AccutaseTM (BioLegends, Paris, France), cells were stained with Fixable Viability Stain 780 (BD Biosciences, Le Pont de Claix, France) for 10 min at room temperature to measure viability. MDM were first blocked in phosphate-buffered saline (PBS) supplemented with 2 % FBS solution and with FcR blocking reagent (Miltenyi Biotec SAS, Paris, France) for 10 min at room temperature to avoid nonspecific binding, and then re-suspended and incubated with specific antibodies or appropriate isotype controls for 30 min at 4°C. Cells were washed with PBS, collected by centrifugation (2500 rpm for 5 min) and then analyzed on a LSR II cytometer (BD Biosciences, San Jose, CA, USA) and FlowLogicTM software (Miltenyi Biotec SAS, Paris, France). The phenotypic characterization of MDMs was performed using the following antibodies: BUV395 anti-MHCII, BV421 anti-CD200R, BV605 anti-

CD80, BB515 anti-CD206, PE anti-CD163 and APC anti-CD86 their respective isotype control, as recommended by BD Biosciences (Le Pont de Claix, France). Results are expressed as the mean ratio of median fluorescence intensity (MFI) calculated as follows: MFI (mAb of interest)/MFI (isotype control mAb).

Phagocytosis assays by flux cytometry

MDMs plated in 12-well tissue culture plates were exposed to fluorescents YG beads (Fluoresbrite™ Plain YG 1.0 Micron Microsphere, Polysciences, Warrington, USA, in a 10:1 ratio (fluorescent beads/MDM) for 45 min at 37°C or 4°C in a 5% CO_2 humidified incubator. Some M0-MDMs were pretreated by 5 µM cytochalasin D (Sigma-Aldrich) for 1 hour, thus acting as a negative control as cytochalasin D inhibits actin polymerization required for engulfment. After phagocytosis, MDMs were washed, detached and stained for viability as already detailed above before YG fluorescence quantification on the cytometer. Results are expressed as % of phagocytosis calculated as follows: % fluorescent MDMs (37°C) - % fluorescent MDMs (4°C).

Efferocytosis Assays by real-time fluorescence microscopy

Human Jurkat CD4 T-lymphocyte cells (1.10^6 cells/ml), cultured in RPMI 1640 Glutamax culture medium with 10 % FBS, 20 IU/ml penicillin and 20 µg/ml streptomycin, were exposed for 4 h to 10 µM camptothecin (Sigma-Aldrich) to induce apoptosis as previously described (Ballerie et al. 2019). Apoptotic Jurkat cells were then stained for 15 min with 250 ng/ml pHrodo (IncuCyte® pHrodo® Red Cell Labeling Kit, Sartorius, Ann Arbor, USA), washed and added to MDMs plated in 96-well-tissue culture plates, in 10:1 ratio (apoptotic cells/MDM) for 180 min at 37◦C in a 5% CO2 humidified incubator. Engulfment efficiency of MDMs was quantified by real-time fluorescence microscopy (IncuCyte® live-cells Analysis system, Sartorius), measuring total integrated red intensity (ex:560nm/em:585nm) of labeled Jurkat cells when entering the acidic phagosome every 15 min. Mean fluorescence intensity of phagocytosed Jurkat cells after 90 min is used to compare the efferocytosis level.

Antinuclear antibodies detection

The anti-nuclear antibodies detection was performed by indirect immunofluorescence technique using HEp-2 (human epithelial cell line) substrate slides and FITC anti-human IgG conjugate (Nova Lite™ Inova Diagnostics, San Diego, USA). Serums were tittered from 1/80 to endpoint. Titrations were expressed as the last positive dilution and aspect were described in accordance to the recommendations from the International Consensus on ANA Patterns (ICAP) group (von Mühlen et al. 2021).

Statistical Analysis

Data are presented as means ± standard error on the mean (SEM). Comparison between more than 2 groups were performed by repeated measure analysis of variance for paired or one-way analysis of variance followed by Dunnett’s or Newman–Keuls multiple comparison post-hoc test. Depending on

conditions and Gaussian distribution, Student's t test, paired-t-test or Mann–Whitney test were used to compare 2 groups. A $P < 0.05$ was considered significant. Data analyzes were performed with GraphPad Prism 5.0 software (GraphPad Software, La Jolla, CA, USA).

Results

Lung and systemic effects of SFA and LFA in mice

Oropharyngeal instillation of LFA resulted in leukocyte accumulation in the airways, which was characterized by a significant increase in neutrophils and macrophages 120-days after fiber exposure. By contrast, no increase in the count number of any leucocyte was found in BAL fluid after SFA exposure (Table 1). In comparison to vehicle- or to SFA-exposed mice, LFA exposure resulted in a significant increase of LDH release (Fig.1a) and of the CCL2/MCP-1 which chemoattracts CCR2 positive monocytes (Fig.1b).

In contrast to SFA, LFA exposure significantly increased tissue inhibitor of matrix metalloproteinase-1 (TIMP-1) release in comparison to control (Fig.1c) denoting of fibrosis development. Exposure to LFA (not SFA) increased hydroxyproline contents when compared to control without reaching a significant level (Fig.1d). As shown in Fig. 1e, LFA exposure induces the development of fibrotic area characterized by less alveolar spaces and alveolar walls thickening than in control and SFA-exposed mice.

As LDH release is associated with cell death, we wondered if LFA-induced dead cells, by releasing cell content in the extracellular microenvironment, exhibit antigenicity and therefore induce a humoral immune response. Therefore, we examined immunoglobulin (Ig) levels in BAL fluids (BALF) of mice. Total IgG and IgM levels did not differ between all groups (Fig.2a). By contrast, mean levels of IgA were significantly increased in BALF of LFA-exposed mice when compared vehicle- or SFA-exposed mice suggesting an activation of lung mucosal immunity (Fig.2a). A significant increase of free DNA levels in BALF (Fig.2b) and of anti-double-stranded (ds-DNA) antibody concentration was observed in the serum of LFA-exposed mice in comparison to control and to SFA-exposed mice (Fig.2c).

Overall, these results demonstrated that contrarily to SFA, inhaled LFA-induced chronic airway inflammation, lung fibrosis, lung mucosal immunity and systemic autoimmunity.

Comparative effects of SFA and LFA fibers on human MDM phenotype and functions

As macrophages are one on the first cell target of inhaled pollutants and as particle exposure may altered the phenotype (M0, M1 and M2) of human MDM (Jaguin et al. 2015), we analyzed the phenotype and the phagocytic functions of MDM exposed to SFA and LFA. The evaluation of fiber toxicity towards human MDM reveals a significant decrease of cell viability in cells exposed for 24 h to 25 $\mu g/cm^2$ and 50 $\mu g/cm^2$ of SFA and FLA respectively (supp data 1). Based on these data, we selected 20 $\mu g/cm^2$ of SFA and LFA for the next in vitro experiments.

A significant down-expression of the endocytic receptor for hemoglobin-haptoglobin complex (or CD163) well known as a M2 marker was found in MDM exposed to SFA and LFA similar to those observed in M1 polarized MDM (Fig.3a). The expression of the MHCII marker was also significantly reduced in the presence of SFA but not with LFA when compared to M0-MDM. No significant alteration of the specific M1 markers CD80 nor the specific M2a marker CD200R were found when MDM were exposed to SFA or LFA (Fig.3a). As the expression of CD86 has a tendency to decrease in SFA-exposed MDM (Fig 3a), we have explored the percentage of cells expressing some M1 markers, and a significant decrease of the percentage of cells positive for both CD86 and MHCII was found in comparison to M0-MDM or LFA-exposed MDM (Fig.3b) suggesting a lower antigen presentation abilities of SFA-exposed MDM.

The quantification of some key pro-inflammatory cytokines showed that the secretion levels of TNFα and IL-8 were significantly induced in supernatants of MDM exposed to SFA and LFA at 20 µg/cm^2 in comparison to M0-MDM, whereas IL-6 secretion was significantly increased only in SFA-exposed MDM when compared to untreated and to LFA-exposed MDM (Fig.4a). The secretion levels of the M2a chemokine CCL18 (Jaguin et al. 2015) was not modified by fiber exposure (data not shown). As asbestos is well known to assemble the NLRP3 inflammasome complex, activating caspase-1 to convert pro-IL-1β to its mature form (Dostert et al. 2008), we compared the effects of particles on the caspase-1 activity and the release of IL-1β from MDMs primed by LPS. Caspase-1 activity (Fig.4b) and the production of IL-1β were induced in LFA-exposed cells (Fig.4c). The secretion of IL-1β in supernatant of SFA-exposed MDM was increased but not enough to reach a significant level. The role of NALP3 inflammasome in IL-1β secretion after LFA exposure was confirmed by the capacity of z-VAD-FMK, a caspase-1 inhibitor, to significantly reduce IL-1β levels (Fig.4c).

As ineffective efferocytosis could contribute to autoimmunity (Kawano and Nagata 2018) and as mineral particles such as crystalline silica decreases efferocytosis capacities of macrophages (Lescoat et al. 2020b), we assessed the effects of asbestos exposure on efferocytosis capacities of macrophages. Human MDM capacities to phagocyte apoptotic cells (efferocytosis) were decreased when exposed to short or long amosite fibers, without significant difference between both fiber types (Fig.5a). By contrast, the phagocytosis of fluorescent beads by MDMs exposed to SFA or to LFA was not reduced, contrarily to those exposed to a potent actin polymerization inhibitor cytochalasin D (Fig.5b).

Altogether, amosite fiber exposure induces a pro-inflammatory phenotype which differs between fiber in IL-6 and IL-1β secretions and that is accompanied for both amosite fibers by a decrease of efferocytosis capacity of human MDM.

Autoimmune effects of crystalline silica and/or asbestos in workers with occupational exposure.

We next determined the links between asbestos exposure, autoimmunity and efferocytosis abilities of MDM obtained from 23 male workers exposed to crystalline silica and/or asbestos fibers, without any known autoimmune diseases. As an association between silica exposure and several autoimmune disorders was previously demonstrated (Pollard 2016) and is well recognized, we used silica-exposed

workers as reference. Antinuclear antibodies (ANA) were detected in the sera from 43,4 % of workers exposed to mineral particles (10 among 23) with the dilution at 1/80 for nine of them and at the dilution 1/320 for one worker exposed to silica. ANA were detected in 71,4% of workers exposed to silica (5 among 7), in 22,2% of workers exposed to asbestos (2 among 9) and in 42,8% of workers co-exposed to asbestos and silica (3 among 7) (Fig.6a). No anti-dsDNA or anti-extractable nuclear antigen (ENA) antibodies were found in the sera of the 23 patients exposed to silicate dusts (data not shown). Lung CT-Scan data have reveals silicosis in two of silica-exposed patients and ANA-positive whereas no lung damage was observed in asbestos-exposed patients (data not shown).

The efferocytosis abilities of MDM from 20 workers exposed to asbestos and/or to crystalline silica did not significantly differ between healthy male donors (HD) (n=11 with a medium of age at 49,9 years) and exposed workers (n=20 with a medium of age at 55,9 years) (Fig.6b). Time of exposure to minerals particles (mean of 20,9 years) had no impact on efferocytosis capacities in exposed workers (data not shown). We also did not observe any difference in the efferocytosis capacities of macrophages according to the positivity of workers for the ANA antibodies using a positivity threshold of 1/80 (Fig.6c).

Altogether, these data confirm the higher link between autoimmunity and crystalline silica exposure in comparison to asbestos exposure and suggest that there is no association between autoimmunity markers and the efferocytosis abilities of MDMs from asbestos-exposed workers.

Discussion

Pathologic responses to toxicant depend on the dose, the duration of exposure and their physical and chemical properties, notably their size. Our study reveals for the first time that the size of amosite fibers has an impact on the development of autoimmunity as only long term LFA-exposed mice had an increased level of anti-dsDNA antibodies. Furthermore, our data support a higher impact of LFA on lung health in comparison of SFA, as LFA exposure was characterized by increased inflammation and higher fibrosis in mice exposed to LFA as compared to mice exposed to SFA. Such differences could be linked to some differences of asbestos-exposed macrophage phenotype and functions.

Asbestos exposure is well known to induce inflammatory responses. In this study, we showed that a long-term exposure to LFA, in contrast to SFA, increased the recruitment of inflammatory cells such as macrophages and more importantly neutrophils in accordance with higher secretion levels of the neutrophil chemoattractive CCL2/MCP-1 chemokine in BALF. This continuing neutrophil response suggests ongoing injury of LFA as compared to SFA that could be related to the insolubility of amphibole in body fluids (Speil and Leineweber 1969) and therefore to their persistency in lung tissue due to “frustrated phagocytosis” by macrophages (Bernstein 2022). Moreover, phagocytosis of long fibers seems aggressive and to favor a high lysosomal membrane rupture and a subsequent release of cathepsin D that results in NLRP3 activation (Li et al. 2012). This is supported by our data showing a better increase of activated-caspase 1 and the process of maturation of pro-IL-1β to the mature and biologically active form of IL-1β by LFA than SFA and by previously studies showing a greater efficiency

of long carbon nanomaterials in comparison to the short, to activate NLRP3 inflammasome in LPS-activated macrophages (Palomäki et al. 2011).

In addition to the secretion of pro-inflammatory markers, human macrophages exposed to SFA and LFA showed, similarly to pro-inflammatory M1 macrophages and to crystalline silica exposure macrophages (Lescoat et al. 2020a), a lower expression of membrane CD163, a scavenger receptor for haptoglobin–hemoglobin complexes. Such a decrease might be due to the over secretion of TNFα after asbestos fibers, a cytokine known to down-regulate CD163 expression in macrophages (Buechler et al. 2000). The pro-inflammatory effects of amosite fiber exposure were confirmed by the over secretion of two major pro-inflammatory markers, IL-8 and IL-6 in human macrophages.

In addition to their inflammatory effects, LFA also induced fibrosis. Extracellular matrix deposit is under the control of mediators such as metalloproteinases and their inhibitors (TIMPs). TIMP-1 overexpression considered as a relevant marker of fibrosis (Manoury et al. 2006) was previously found increased after chrysotile inhalation in mice (Sabo-Attwood et al. 2011). Such an increase of TIMP-1 in BALF of LFA-exposed mice supports the idea that a non-degrading extracellular matrix environment favor fibrosis. The higher capacity of long asbestos fibers to increase lung fibrosis in comparison to short fibers confirmed previous histopathologic data collected in rodents exposed to amosite (Davis et al. 1986) or crocidolite fibers (Adamson and Bowden 1987).

In addition to pulmonary disorders, exposure to amphibole favors autoimmunity in human and mice but, to our knowledge, the role of the size of the fibers was not evaluated. Notably, because of the difficulties to characterize the size and the shape of the amosite fibers to which workers are exposed, in the epidemiological studies. In addition to the inflammatory and fibrotic effects of long amosite fibers that might as the result of cell injury attested by LDH and free DNA release in BALF, the presence of free DNA represents a possible source of autoantigens (Soni and Reizis 2018). Such hypothesis is supported by data showing that an impaired DNase I activity has increased the production of autoantibodies in systemic lupus erythematosus (Gajic-Veljic et al. 2015), an autoimmune disease for which crystalline silica is a risk factor, knowing that crystalline silicate exposure induced self-dsDNA release in lung (Benmerzoug et al. 2018). The development of an adaptive response is favored by the presence of danger signals such as pollutants that can promote a breakdown in tolerance, and also depends on the nature of the antigens associated with such danger signals. The presence of cell corpses related to an increase of apoptosis and/or a decrease of cell clearance favors autoimmunity (Abdolmaleki et al. 2018; Kawano and Nagata 2018). Asbestos induce apoptosis (Hamilton et al. 1996; Liu et al. 2000) and the decrease of efferocytosis that we observed in macrophages exposed to amosite fibers might therefore favors inflammation by both decreasing the pro-resolutive effects of efferocytic cells secreting IL-10 and by increasing the secondary necrosis followed by damage signal release. Secondary necrosis may also favor autoimmune responses after the release of auto-antigens such as DNA or nuclear proteins. The increase of seric anti-dsDNA antibodies found in LFA- (not SFA) exposed mice is an accordance with the increase of free DNA that we observed and confirms the production of systemic autoimmune markers related to cell damage. Such data are also in accordance with a study showing that individuals exposed

to asbestos fibers showed more DNA double-strand breaks in white blood cells and higher blood levels of anti-dsDNA antibodies than non-exposed subjects (Marczynski et al. 1994b). Moreover, the higher autoimmune potential of LFA that we observed might also be related to the greater oxidizing potential of LFA in comparison to SFA (Tomatis et al. 2010). Indeed, ROS can generate oxidized protein that may cause immunogenic reactions by inducing pathogenic antibody release in systemic diseases such as systemic sclerosis (Servettaz et al. 2009).

Antigenicity is not sufficient to elicit adaptive immunity. The presentation of antigenic peptides to T cells requires the expression of co-stimulatory molecules on antigen-presenting cells. As we observed a significant decrease of MHCII and CD86 expression by SFA-exposed macrophages, we may hypothesize that their ability to present antigen and to activate T cells were reduced and explain the lower immunoglobulin levels in BALF of SFA-exposed mice when compared to LFA-exposed mice.

Asbestos-induced disorders of autoimmunity can also be explained by adjuvant-type and inflammatory effects of asbestos as it was also demonstrated for crystalline silica (Otsuki et al. 2007; Dostert et al. 2008). The activation of macrophages by the internalization of silicate compounds, favors the secretion of IL1-β-dependent inflammasome activation and others inflammatory markers that can then activate T-Helper cells that facilitate B-cell production of antibodies (Eisenbarth et al. 2008). The moderate higher capacity of LFA to activate NLRP3 inflammasome an IL-1β secretion in comparison to SFA suggests a superior adjuvant effect of long fibers.

IgA are produced by B cells in mucosal immune systems following interaction between T cells and antigen presentative cells that have taken up and process specific antigen (Corthésy 2013). The specific and strong increase of IgA levels in BALF of mice exposed to LFA suggested an activation of mucosa-associated lymphoid tissue by long amosite fibers but not by short ones. Such an increase of IgA secretion was previously observed in the sera of a population exposed to Libby amphibole fibers (Pfau et al. 2005). An increase of IgA levels was also found in the serum and BALF of silica-inhaled lupus prone mice (Rajasinghe et al. 2020) confirming, here again, the use of common defense mechanisms between these two dusts.

Association between amphibole exposure, ANA positivity and the frequency of rheumatologic diseases has been reported (Pfau et al. 2005; Parks and Cooper 2005). In our study, 43 % of occupationally exposed workers had a low positive ANA titer (1/80) that is usually not considered as a positive threshold for autoimmunity but that has nonetheless been endorsed for the diagnosis of systemic lupus (Aringer et al. 2019). Moreover, workers included in our study have neither anti-DNA or anti-ENA antibody positivity nor any diagnosis of systemic autoimmunity, whereas positivity of anti-dsDNA occurs in more than 70 % of patients with autoimmune systemic lupus (Lou et al. 2022). These observations suggest that none of the workers included in our work had clinically meaningful autoimmune markers at the time of the analysis. Even if ANA levels were low, our data confirm the higher risk factor of autoimmunity after a silica exposure in comparison to asbestos. As a decrease of efferocytosis abilities of MDMs was previously described in autoimmune diseases such as systemic lupus (Tas et al. 2006), Sjogren's

disease (Manoussakis et al. 2014) and systemic sclerosis (Ballerie et al. 2019) with significant ANA positivity, it was not surprising that macrophages from workers included in our study, with low titters of ANA did not present a defect of apoptotic cell clearance. As immune alteration may precede the onset of asbestos-related lung disease (Pfau et al. 2011; Bellando-Randone et al. 2022), it would be interesting to follow these 23 patients to assess the onset of autoimmune features or lung damages, as detected by routine CT-scan.

Altogether, we hypothesize that autoimmune effects of LFA may be sequenced first by cell death associated with a defect of efferocytosis that favors an accumulation of residual cell corpses and a subsequent secondary necrosis, which represents a source of autoantigen and, second to an immune activation via the adjuvant effect (NLRP3 inflammasome) of long fibers, leading to antigens presentation. Such pathogenic events could elicit an elevation of local IgA and systemic autoantibody production, favor by the chronic persistence of LFA in the lung (Fig.7).

Overall, our results confirmed the higher lung pathogenicity of LFA as compared SFA in mouse model. So, we highlighted that the size of amosite fiber represents a key parameter to assess the risk of developing systemic autoimmunity. Careful assessment of autoimmune features in patients exposed to LFA might be proposed for early detection of the disease and early treatment, before irreversible damages appear.

Declarations

Ethics approval and consent to participate

Both human serum samples and animal studies were approved by the Committee for protection of persons (approval Ile de France 5, N°2020-A01990-39) and the Institutional Animal Care and Use Committee (EEC n°86/609, LA1230312 and 2018/UCL/MD/012), respectively.

Availability of data and material

The datasets generated during and/or analysed during the current study are available from the corresponding author on reasonable request.

Competing interests

The authors have no conflict of interest to declare.

Funding

This work was supported by the « Agence Nationale de sécurité sanitaire de l'alimentation, de l'environnement et du travail » (Anses) (MacFibOsis project N°2018/1/149), the Institut National de la Santé et de la Recherche Médicale (INSERM), the Université de Rennes (Univ Rennes), « Actions de Recherche Concertées, Fédération Wallonie-Bruxelles (ARC 19/24-098, CYTAID), « Fondation Contre le Cancer » (2019-219), and European Commission under H2020 project (Contract no. 874707,

Eximious). FT kindly acknowledges the financial support from BRIC 2019 project “Caractterizzazione cristallochimica e studio della reattività de superficie di fibre menerali di interesse ambiantale e sanitario ai fini di un’accurata analisa del rischio di contaminazione » funded by INAIL with Grant number ID 57.1. FH is a Senior Research Associate with the FNRS, Belgium.

Author’s contributions

“The authors that contributed to the study conception and design were AL, FH and VL. Material preparation, data collection and analysis were performed by AL, RL, KP, YY, FT, CP, AP, NB, ML, ELT, ED, FH and VL*. The first draft of the manuscript was written by VL and AL and all authors commented on previous versions of the manuscript. All authors read and approved the final manuscript.”*

Acknowledgements

The authors thank the platform of Flow cytometry (Biosit, Rennes, France) and the nurses, medical team and the patients from the “Service de Santé au Travail et Pathologie Professionnelle” and V. Visseiche and K. Coat of Rennes Hospital (France).

References

1. Abdolmaleki F, Farahani N, Gheibi Hayat SM, et al (2018) The Role of Efferocytosis in Autoimmune Diseases. Front Immunol 9:1645. https://doi.org/10.3389/fimmu.2018.01645
2. Adamson IY, Bowden DH (1987) Response of mouse lung to crocidolite asbestos. 1. Minimal fibrotic reaction to short fibres. J Pathol 152:99–107. https://doi.org/10.1002/path.1711520206
3. Aringer M, Costenbader K, Daikh D, et al (2019) 2019 European League Against Rheumatism/American College of Rheumatology Classification Criteria for Systemic Lupus Erythematosus. Arthritis Rheumatol 71:1400–1412. https://doi.org/10.1002/art.40930
4. Arras M, Huaux F, Vink A, et al (2001) Interleukin-9 reduces lung fibrosis and type 2 immune polarization induced by silica particles in a murine model. Am J Respir Cell Mol Biol 24:368–375. https://doi.org/10.1165/ajrcmb.24.4.4249
5. Ballerie A, Lescoat A, Augagneur Y, et al (2019) Efferocytosis capacities of blood monocyte-derived macrophages in systemic sclerosis. Immunol Cell Biol 97:340–347. https://doi.org/10.1111/imcb.12217
6. Bellando-Randone S, Del Galdo F, Matucci-Cerinic M (2022) Insights into molecular and clinical characteristics of very early systemic sclerosis. Curr Opin Rheumatol 34:351–356. https://doi.org/10.1097/BOR.0000000000000903
7. Benmerzoug S, Rose S, Bounab B, et al (2018) STING-dependent sensing of self-DNA drives silica-induced lung inflammation. Nat Commun 9:5226. https://doi.org/10.1038/s41467-018-07425-1
8. Bernstein DM (2022) The health effects of short fiber chrysotile and amphibole asbestos. Crit Rev Toxicol 52:89–112. https://doi.org/10.1080/10408444.2022.2056430

9. Biondi PA, Chiesa LM, Storelli MR, Renon P (1997) A new procedure for the specific high-performance liquid chromatographic determination of hydroxyproline. J Chromatogr Sci 35:509–512. https://doi.org/10.1093/chromsci/35.11.509
10. Boulanger G, Andujar P, Pairon J-C, et al (2014) Quantification of short and long asbestos fibers to assess asbestos exposure: a review of fiber size toxicity. Environ Health 13:59. https://doi.org/10.1186/1476-069X-13-59
11. Buechler C, Ritter M, Orsó E, et al (2000) Regulation of scavenger receptor CD163 expression in human monocytes and macrophages by pro- and antiinflammatory stimuli. J Leukoc Biol 67:97–103
12. Bunderson-Schelvan M, Pfau JC, Crouch R, Holian A (2011) Nonpulmonary outcomes of asbestos exposure. J Toxicol Environ Health B Crit Rev 14:122–152. https://doi.org/10.1080/10937404.2011.556048
13. Cavalin C, Lescoat A, Sigaux J, et al (2022) Crystalline silica exposure in patients with rheumatoid arthritis and systemic sclerosis: a nationwide cross-sectional survey. Rheumatology (Oxford) keac675. https://doi.org/10.1093/rheumatology/keac675
14. Corthésy B (2013) Multi-faceted functions of secretory IgA at mucosal surfaces. Front Immunol 4:185. https://doi.org/10.3389/fimmu.2013.00185
15. Davis JM, Addison J, Bolton RE, et al (1986) The pathogenicity of long versus short fibre samples of amosite asbestos administered to rats by inhalation and intraperitoneal injection. Br J Exp Pathol 67:415–430
16. Dostert C, Pétrilli V, Van Bruggen R, et al (2008) Innate immune activation through Nalp3 inflammasome sensing of asbestos and silica. Science 320:674–677. https://doi.org/10.1126/science.1156995
17. Eisenbarth SC, Colegio OR, O'Connor W, et al (2008) Crucial role for the Nalp3 inflammasome in the immunostimulatory properties of aluminium adjuvants. Nature 453:1122–1126. https://doi.org/10.1038/nature06939
18. Gajic-Veljic M, Bonaci-Nikolic B, Lekic B, et al (2015) Importance of low serum DNase I activity and polyspecific anti-neutrophil cytoplasmic antibodies in propylthiouracil-induced lupus-like syndrome. Rheumatology (Oxford) 54:2061–2070. https://doi.org/10.1093/rheumatology/kev243
19. Hamilton RF, Iyer LL, Holian A (1996) Asbestos induces apoptosis in human alveolar macrophages. Am J Physiol 271:L813-819. https://doi.org/10.1152/ajplung.1996.271.5.L813
20. Jaguin M, Fardel O, Lecureur V (2015) Exposure to diesel exhaust particle extracts (DEPe) impairs some polarization markers and functions of human macrophages through activation of AhR and Nrf2. PLoS One 10:e0116560. https://doi.org/10.1371/journal.pone.0116560
21. Janssen LMF, Ghosh M, Lemaire F, et al (2022) Exposure to silicates and systemic autoimmune-related outcomes in rodents: a systematic review. Part Fibre Toxicol 19:4. https://doi.org/10.1186/s12989-021-00439-6
22. Joshi N, Watanabe S, Verma R, et al (2020) A spatially restricted fibrotic niche in pulmonary fibrosis is sustained by M-CSF/M-CSFR signalling in monocyte-derived alveolar macrophages. Eur Respir J

55:1900646. https://doi.org/10.1183/13993003.00646-2019

23. Kawano M, Nagata S (2018) Efferocytosis and autoimmune disease. Int Immunol 30:551–558. https://doi.org/10.1093/intimm/dxy055
24. Lescoat A, Ballerie A, Lelong M, et al (2020a) Crystalline Silica Impairs Efferocytosis Abilities of Human and Mouse Macrophages: Implication for Silica-Associated Systemic Sclerosis. Front Immunol 11:219. https://doi.org/10.3389/fimmu.2020.00219
25. Lescoat A, Lelong M, Jeljeli M, et al (2020b) Combined anti-fibrotic and anti-inflammatory properties of JAK-inhibitors on macrophages in vitro and in vivo: Perspectives for scleroderma-associated interstitial lung disease. Biochem Pharmacol 178:114103. https://doi.org/10.1016/j.bcp.2020.114103
26. Li M, Gunter ME, Fukagawa NK (2012) Differential activation of the inflammasome in THP-1 cells exposed to chrysotile asbestos and Libby “six-mix” amphiboles and subsequent activation of BEAS-2B cells. Cytokine 60:718–730. https://doi.org/10.1016/j.cyto.2012.08.025
27. Liu W, Ernst JD, Broaddus VC (2000) Phagocytosis of crocidolite asbestos induces oxidative stress, DNA damage, and apoptosis in mesothelial cells. Am J Respir Cell Mol Biol 23:371–378. https://doi.org/10.1165/ajrcmb.23.3.4094
28. Lou H, Ling GS, Cao X (2022) Autoantibodies in systemic lupus erythematosus: From immunopathology to therapeutic target. J Autoimmun 102861. https://doi.org/10.1016/j.jaut.2022.102861
29. Manoury B, Caulet-Maugendre S, Guénon I, et al (2006) TIMP-1 is a key factor of fibrogenic response to bleomycin in mouse lung. Int J Immunopathol Pharmacol 19:471–487. https://doi.org/10.1177/039463200601900303
30. Manoussakis MN, Fragoulis GE, Vakrakou AG, Moutsopoulos HM (2014) Impaired clearance of early apoptotic cells mediated by inhibitory IgG antibodies in patients with primary Sjögren’s syndrome. PLoS One 9:e112100. https://doi.org/10.1371/journal.pone.0112100
31. Marczynski B, Czuppon AB, Marek W, et al (1994a) Increased incidence of DNA double-strand breaks and anti-ds DNA antibodies in blood of workers occupationally exposed to asbestos. Hum Exp Toxicol 13:3–9. https://doi.org/10.1177/096032719401300102
32. Marczynski B, Czuppon AB, Marek W, et al (1994b) Increased incidence of DNA double-strand breaks and anti-ds DNA antibodies in blood of workers occupationally exposed to asbestos. Hum Exp Toxicol 13:3–9. https://doi.org/10.1177/096032719401300102
33. Murthy S, Larson-Casey JL, Ryan AJ, et al (2015) Alternative activation of macrophages and pulmonary fibrosis are modulated by scavenger receptor, macrophage receptor with collagenous structure. FASEB J 29:3527–3536. https://doi.org/10.1096/fj.15-271304
34. Otsuki T, Maeda M, Murakami S, et al (2007) Immunological effects of silica and asbestos. Cell Mol Immunol 4:261–268
35. Palomäki J, Välimäki E, Sund J, et al (2011) Long, needle-like carbon nanotubes and asbestos activate the NLRP3 inflammasome through a similar mechanism. ACS Nano 5:6861–6870.

https://doi.org/10.1021/nn200595c

36. Parks CG, Conrad K, Cooper GS (1999) Occupational exposure to crystalline silica and autoimmune disease. Environ Health Perspect 107 Suppl 5:793–802. https://doi.org/10.1289/ehp.99107s5793
37. Parks CG, Cooper GS (2005) Occupational exposures and risk of systemic lupus erythematosus. Autoimmunity 38:497–506. https://doi.org/10.1080/08916930500285493
38. Pfau JC, Li S, Holland S, Sentissi JJ (2011) Alteration of fibroblast phenotype by asbestos-induced autoantibodies. J Immunotoxicol 8:159–169. https://doi.org/10.3109/1547691X.2011.562257
39. Pfau JC, Sentissi JJ, Weller G, Putnam EA (2005) Assessment of autoimmune responses associated with asbestos exposure in Libby, Montana, USA. Environ Health Perspect 113:25–30. https://doi.org/10.1289/ehp.7431
40. Pfau JC, Serve KM, Noonan CW (2014) Autoimmunity and asbestos exposure. Autoimmune Dis 2014:782045. https://doi.org/10.1155/2014/782045
41. Pollard KM (2016) Silica, Silicosis, and Autoimmunity. Front Immunol 7:. https://doi.org/10.3389/fimmu.2016.00097
42. Rajasinghe LD, Li Q-Z, Zhu C, et al (2020) Omega-3 fatty acid intake suppresses induction of diverse autoantibody repertoire by crystalline silica in lupus-prone mice. Autoimmunity 53:415–433. https://doi.org/10.1080/08916934.2020.1801651
43. Sabo-Attwood T, Ramos-Nino ME, Eugenia-Ariza M, et al (2011) Osteopontin modulates inflammation, mucin production, and gene expression signatures after inhalation of asbestos in a murine model of fibrosis. Am J Pathol 178:1975–1985. https://doi.org/10.1016/j.ajpath.2011.01.048
44. Servettaz A, Goulvestre C, Kavian N, et al (2009) Selective oxidation of DNA topoisomerase 1 induces systemic sclerosis in the mouse. J Immunol 182:5855–5864. https://doi.org/10.4049/jimmunol.0803705
45. Soni C, Reizis B (2018) DNA as a self-antigen: nature and regulation. Curr Opin Immunol 55:31–37. https://doi.org/10.1016/j.coi.2018.09.009
46. Speil S, Leineweber JP (1969) Asbestos minerals in modern technology. Environ Res 2:166–208. https://doi.org/10.1016/0013-9351(69)90036-x
47. Tas SW, Quartier P, Botto M, Fossati-Jimack L (2006) Macrophages from patients with SLE and rheumatoid arthritis have defective adhesion in vitro, while only SLE macrophages have impaired uptake of apoptotic cells. Ann Rheum Dis 65:216–221. https://doi.org/10.1136/ard.2005.037143
48. Tomatis M, Turci F, Ceschino R, et al (2010) High aspect ratio materials: role of surface chemistry vs. length in the historical “long and short amosite asbestos fibers.” Inhal Toxicol 22:984–998. https://doi.org/10.3109/08958378.2010.504243
49. von Mühlen CA, Garcia-De La Torre I, Infantino M, et al (2021) How to report the antinuclear antibodies (anti-cell antibodies) test on HEp-2 cells: guidelines from the ICAP initiative. Immunol Res 69:594–608. https://doi.org/10.1007/s12026-021-09233-0

50. Webber MP, Moir W, Zeig-Owens R, et al (2015) Nested case-control study of selected systemic autoimmune diseases in World Trade Center rescue/recovery workers. Arthritis Rheumatol 67:1369–1376. https://doi.org/10.1002/art.39059
51. Zebedeo CN, Davis C, Peña C, et al (2014) Erionite induces production of autoantibodies and IL-17 in C57BL/6 mice. Toxicol Appl Pharmacol 275:257–264. https://doi.org/10.1016/j.taap.2014.01.018

Tables

Table 1 : Cell counts in the BAL fluids from mice after 120 days of oropharyngeal instillation of SFA, LFA or NaCl (Control)

	mean ± SEM	differential cell counts (number 103/ml)			
group	Total cell number (106/ml)	Macrophages	Neutrophils	Lymphocytes	Eosinophils
after 120 days					
NaCl	31,0 + 2,7	28.8 + 2,4	1,7 + 0,6	0	nd
SFA	31,2 + 4,2	28,0 + 3,5	2,7 + 0,5	0,5 + 0,2	nd
LFA	73,0 + 18,1 *$	59,2 + 14,9 *$	10,2 + 3,1**$	1,1 + 0,6	nd
* significantly different (p<0.05) from NaCl control					
** significantly different (p<0,01) from NaCl control					
$ significantly different (p<0.05) from SFA					
nd: not detected					

Figures

Fig. 1

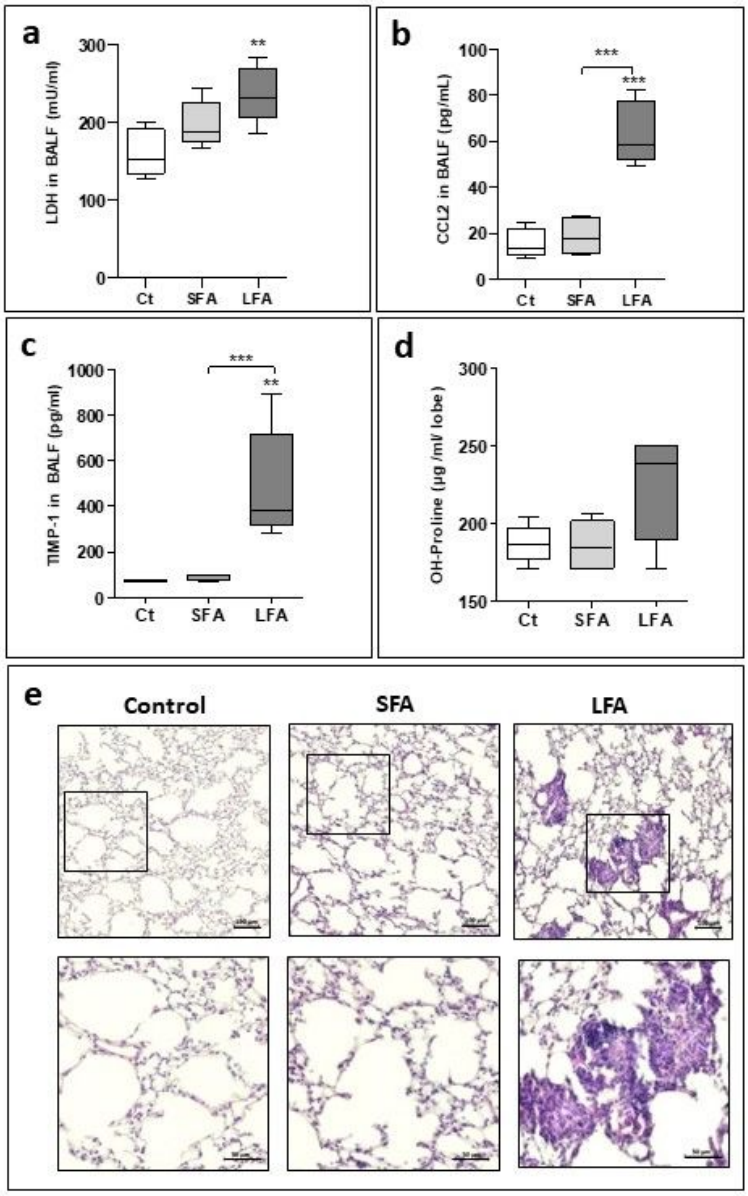

Figure 1

Comparison of SFA and LFA exposure on lung inflammation and fibrosis. BAL fluids and lung were harvested at day 120 from control-, SFA- or LFA-treated mice and analyzed for LDH release expressed in mU/ml (a), CCL2 (b) and TIMP-1 (c) secretions expressed in pg/ml and for hydroxyproline content expressed in µg/ml/lobe (d). Data represented the mean ± SEM with n=5. **p<0.01, ***p<0.001.

Microscopic views of representative lung sections from control-, short or long amosite fibers at day 120, using bright light (e).

Fig. 2

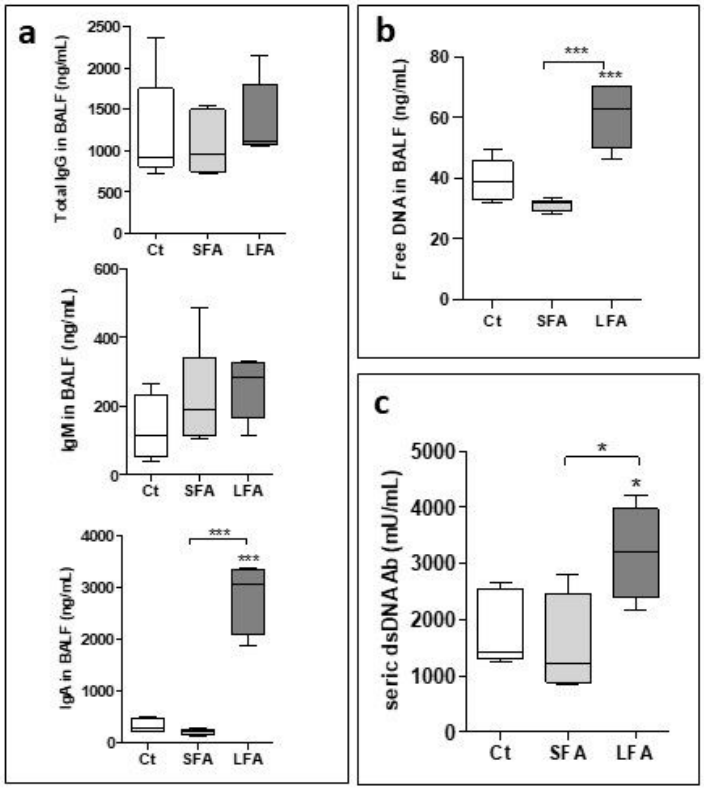

Figure 2

Comparison of immune response to SFA and LFA exposure. BAL fluids and lung tissue were harvested at day 120 from control-, SFA- or LFA-treated mice and analyzed for immunoglobulin IgG, IgA and IgM (a)

and for free DNA content expressed in ng/ml (b). Double-strand DNA antibodies concentrations, expressed in mU/ml, were analyzed in the sera of mice (c). Data represented the mean ± SEM with n=5. *p<0.05, ***p<0.001.

Fig. 3

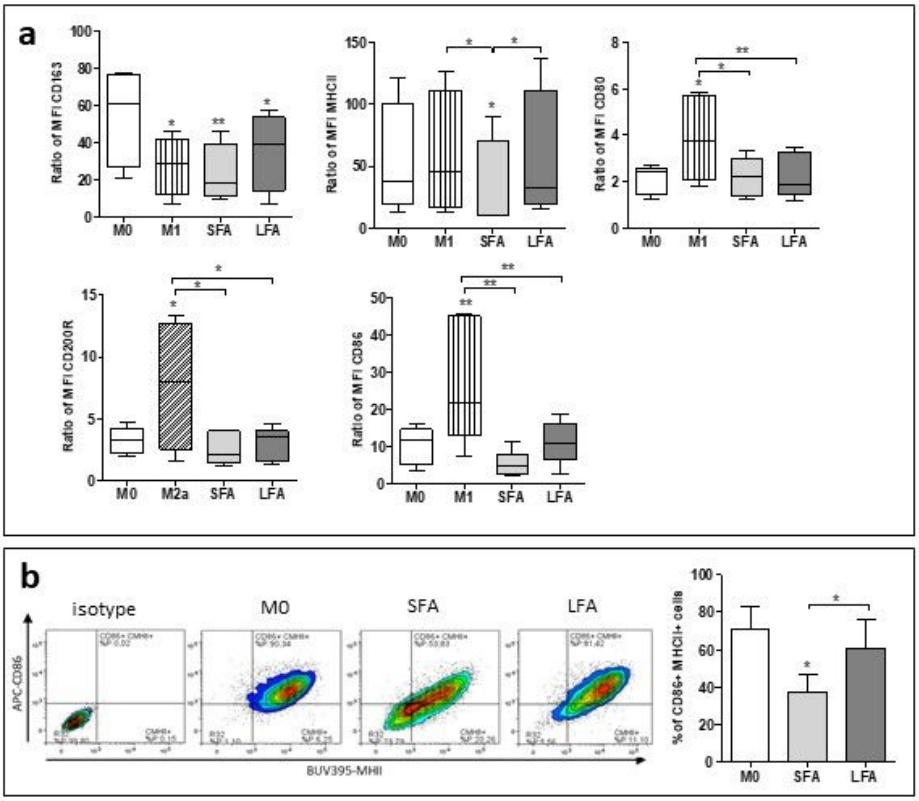

Figure 3

Expression of polarization markers of monocyte-derived macrophages (MDMs) exposed to SFA and LFA. MDMs were polarized for 24 h by addition of IFNγ/LPS (M1) or IL-4/IL-13 (M2a) or to unpolarized control cells (M0). In parallel, M0-MDMs were exposed to 20 μg/cm^2 of SFA or LFA for 24 h. Cells were harvested, stained and the expression of cell surface molecules was analyzed by flow cytometry. Data are expressed as MFI relative to isotype control (ratio) ± SEM for 4-5 independents experiments (a). Representative graph from flow cytometry showing the co-expression of CD86 and MHCII in M0 exposed or not to SFA and LFA (b). Data are expressed as the percentage of co-expressing cells ± SEM for 4 independents experiments (b). *p<0.05, **p<0.01.

Fig. 4

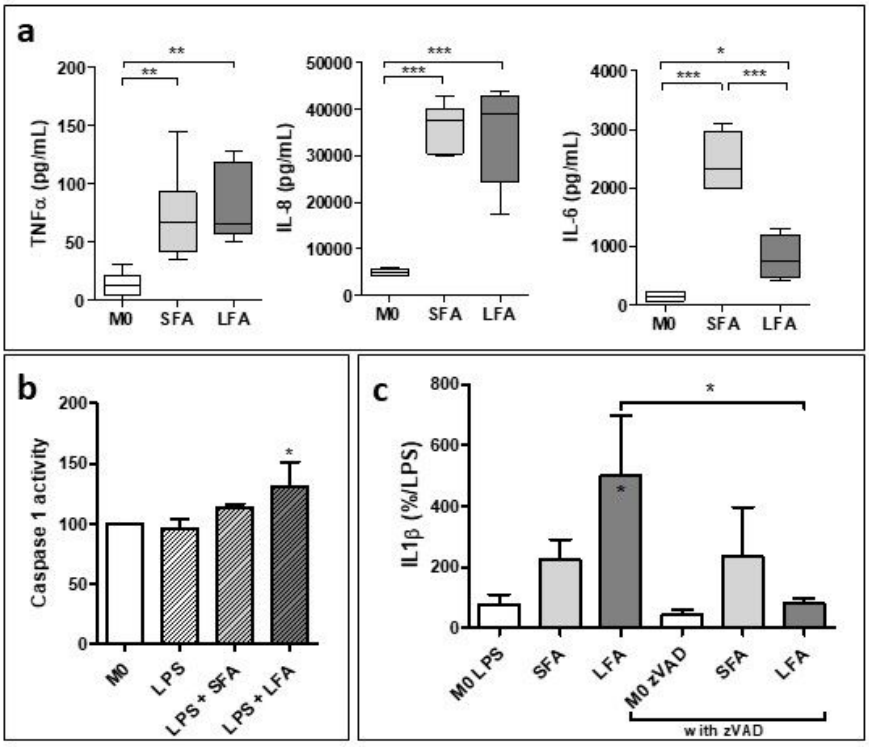

Figure 4

Comparison of inflammatory response of monocyte-derived macrophages (MDMs) exposed to SFA and LFA. MDMs were exposed to SFA or LFA at 20 µg/cm^2 for 24 h. Supernatants were harvested and analyzed by ELISA to determine the concentrations of some cytokines/chemokines. Data expressed in pg/ml, represent the mean ± SEM of at least 4 independent experiments (a). MDM were pre-treated for 4 h with LPS (10 ng/ml) in the presence of the caspase 1 inhibitor z-vad-FMK (10 µM) (c) before to be

exposed to SFA or LFA at 20 µg/cm^2 for 2 h for the analysis of caspase-1 activity (b) or for 18 h for the determination of the IL-1β concentration by ELISA (c) as described in Materials and methods. Data expressed in percentage relative to untreated cells (M0) were the mean ± SEM of 5 independent experiments (b). Data expressed in percentage of LPS-activated control cells represent the mean ± SEM of 3 independent experiments (c). *p<0.05, **p<0.01, ***p<0.001.

Fig. 5

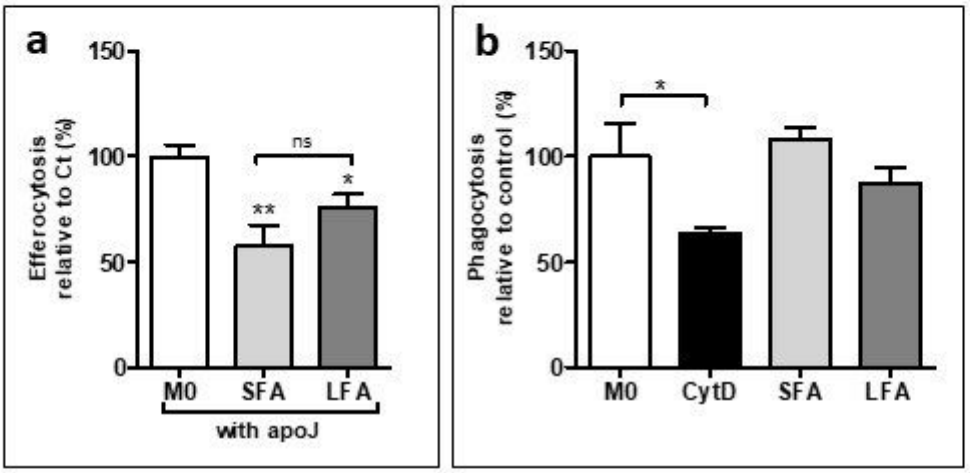

Figure 5

Comparison of SFA and LFA exposure of human macrophages on efferocytosis and phagocytosis. Monocyte-derived macrophages (MDMs) were exposed to SFA or LFA at 20 µg/cm^2 for 4 h, were then exposed to apoptotic Jurkat (apoJ) cells as described in the Materials and methods to evaluate their efferocytosis abilities. Data expressed in percentage relative to untreated cells (M0) were the mean ± SEM

of 5 independent experiments (a). MDMs were exposed to SFA or LFA at 20 µg/cm^2 for 4 h or to cytochalasin D (cytD) at for 1 h and then exposed to fluorescent beads for 45 min as described in the Materials and methods. Data expressed in percentage relative to untreated cells (M0) were the mean ± SEM of 6 independent experiments (b). *p<0.05, **p<0.01.

Fig. 6

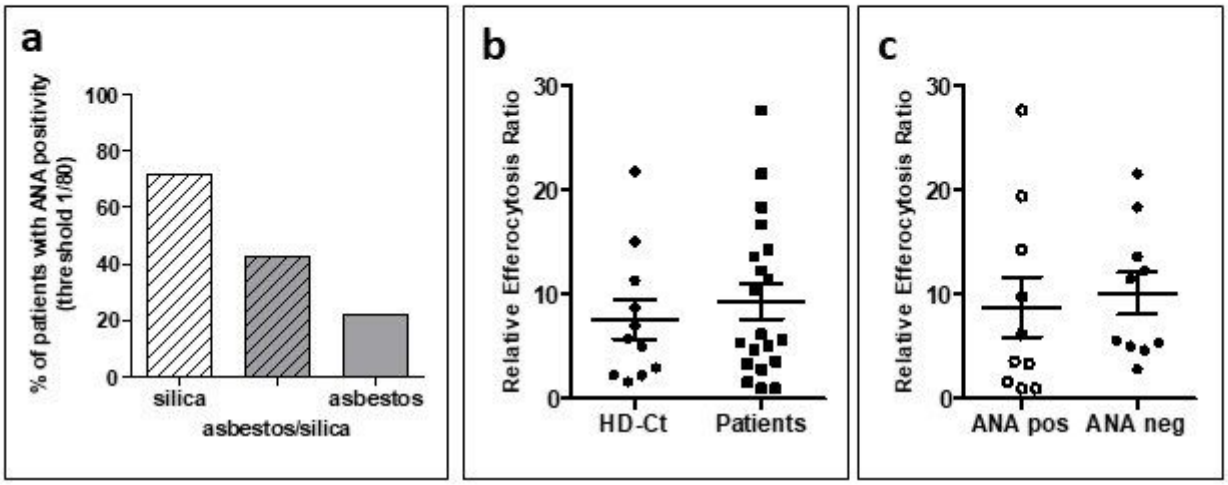

Figure 6

Evaluation of autoimmunity and efferocytosis abilities of MDMs of workers with occupational exposure to asbestos and/or crystalline silicate. The percentage of patients (n=23) with ANA positivity (with a threshold 1/80) was evaluated in sera of patients as described in materials and methods (a). Monocyte-derived macrophages (MDMs) from patients occupationally exposed to asbestos and/or crystalline silica were exposed to apoptotic Jurkat (apoJ) cells as described in the Materials and methods to evaluate their efferocytosis abilities. Data expressed as relative efferocytosis ratio, determined as follow (mean

fluorescence intensity of patients MDM/ mean fluorescence intensity of patients MDM + cytochalasin D, an inhibitor of actin polymerization, used to determine a baseline), compare the efferocytosis abilities of MDMs from HD and patients (b) and of patients ANA positive and ANA negative (c).

Fig.7

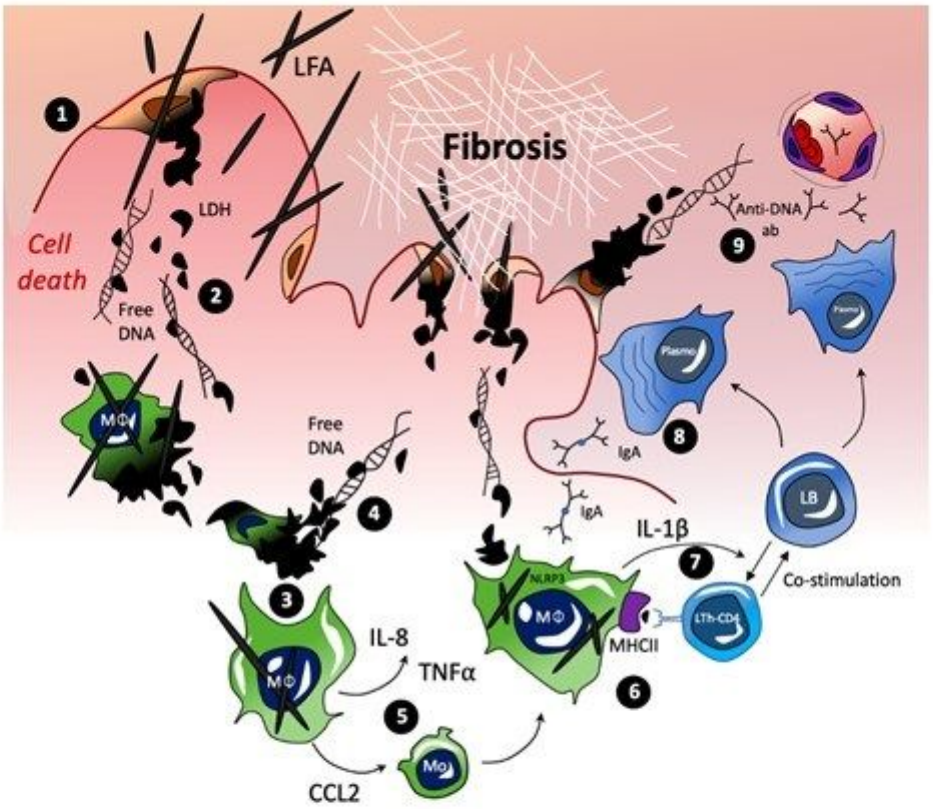

Figure 7

Autoimmune effects of LFA could be triggered by: (1) LFA-induced cell death associated with (2) a release of autoantigens and free DNA, favored by (3) a defect of efferocytosis leading to an (4) accumulation of

residual cell corpses with secondary necrosis. LFA also induced (5) the release of IL-8 and TNFα by macrophages (M), and CCL-2 in the alveolar lumen, with potential recruitment of monocytes (Mo), increasing lung inflammation. Autoantigens can be (6) presented to lymphocyte Th-CD4 through MHCII, since its expression is preserved after LFA exposure by contrast to SFA exposure. Immune activation after LFA exposure is also favored by (7) the adjuvant effect (NLRP3 inflammasome) of LFA, leading to a release of IL-1β. Such pathogenic events could elicit an elevation of (8) local IgA in the lungs and (9) systemic autoantibody production, favored by the chronic persistence of LFA in the lung.

Supplementary Files

This is a list of supplementary files associated with this preprint. Click to download.

- LescoatSuppdata2nov22Archives.pptx